Supplement of Atmos. Chem. Phys., 14, 9695–9706, 2014
http://www.atmos-chem-phys.net/14/9695/2014/
doi:10.5194/acp-14-9695-2014-supplement

Atmospheric Chemistry and Physics Open Access

Supplement of

Aqueous-phase photooxidation of levoglucosan – a mechanistic study using aerosol time-of-flight chemical ionization mass spectrometry (Aerosol ToF-CIMS)

R. Zhao et al.

Correspondence to: J. P. D. Abbatt (jabbatt@chem.utoronto.ca)

Table S1: List of peaks detected by the $I(H_2O)_n^-$ reagent ion. The chemical formulae were assigned using the data processing software (Tofwerk v. 2.2). The peak time and Max. peak intensity are the illumination time at which each peak reached its maximum, and its corresponding signal intensity at that time, respectively. The peak intensity has been normalized by the intensity of the reagent ion at m/z 145 ($I(H_2O)^-$). This information, along with the exact m/z and mass defect were used to construct the mass defect plot (Figure 4 in the main article). The compounds displayed in Figure 6 in the main article are color coded.

Detected Formula	Exact m/z (Th)	Mass defect (Th)	Peak time (min)	Max. peak intensity	Note
CH2O2I	172.911	-0.0895	133	5.76E-03	Formic acid
C2H2O3I	200.905	-0.09458	300	7.91E-03	glyoxylic acid
C2H4O3I	202.921	-0.07893	300	2.92E-03	glycolic acid or glyoxal monohydrate
C3H2O3I	212.905	-0.09458	145	1.82E-03	Product (i)
C3H4O3I	214.921	-0.07893	95	7.51E-04	Product (ii)
C2H2O4I	216.900	-0.09967	500	3.00E-03	Oxalic acid
C3H6O3I	216.937	-0.06328	62	1.97E-03	
C2H4O4I	218.916	-0.08402	83	1.05E-04	
C4H4O3I	226.921	-0.07893	105	1.42E-04	
C4H4O3I	226.921	-0.07893	105	1.42E-04	
C3H2O4I	228.900	-0.09967	200	8.57E-05	
C4H6O3I	228.937	-0.06328	90	3.27E-04	
C3H4O4I	230.916	-0.08402	182	6.38E-04	
C3H6IO4	232.932	-0.06837	141	9.79E-05	
C5H4IO3	238.921	-0.07893	97	2.64E-04	
C4H2O4I	240.900	-0.09967	101	2.46E-03	
C4H4O4I	242.916	-0.08402	105	9.02E-04	
C4H6O4I	244.932	-0.06837	79	1.05E-03	Product (iii)
C3H4IO5	246.911	-0.0891	233	6.81E-05	
C5H2IO4	252.900	-0.09967	97	1.40E-04	
C5H4O4I	254.916	-0.08402	98	2.73E-04	
C4H2O5I	256.895	-0.10475	200	4.00E-05	
C5H6O4I	256.932	-0.06837	95	3.29E-04	
C4H4O5I	258.911	-0.0891	169	9.14E-04	Product (iv)
C5H8O4I	258.947	-0.05272	66	2.65E-04	
C4H6O5I	260.927	-0.07345	97	1.37E-04	
C3H4IO6	262.906	-0.09419	500	4.00E-05	
C5H2O5I	268.895	-0.10475	160	1.40E-04	
C5H4IO5	270.911	-0.0891	116	3.79E-04	
C5H6IO5	272.927	-0.07345	75	1.31E-03	Product (v)
C5H8IO5	274.942	-0.0578	72	2.33E-04	Product (vi)
C4H6IO6	276.921	-0.07854	151	4.37E-05	
C6H4IO5	282.911	-0.0891	102	7.21E-05	
C6H6O5I	284.927	-0.07345	76	1.02E-03	

C6H8IO5	286.942	-0.0578	48	6.49E-03	
C6H10IO5	**288.958**	**-0.04215**	**0**	**4.49E-02**	**levoglucosan**
C6H2O6I	296.890	-0.10984	260	3.80E-05	
C6H4O6I	298.906	-0.09419	136	1.80E-04	
C6H6O6I	300.921	-0.07854	97	1.19E-03	
C6H8O6I	302.937	-0.06289	81	7.67E-04	
C6H10O6I	304.953	-0.04724	46	5.08E-04	
C6H4O7I	314.901	-0.09927	220	3.33E-05	
C6H6IO7	316.916	-0.08362	200	1.85E-04	
C6H8O7I	318.932	-0.06797	97	5.93E-04	
C5H6O8I	320.911	-0.08871	330	4.00E-05	
C6H10IO7	320.948	-0.05232	59	4.83E-04	Product (vii)
C6H6O8I	332.911	-0.08871	280	8.00E-05	
C6H8O8I	334.927	-0.07306	143	1.78E-04	
C6H10O8I	336.943	-0.05741	61	1.34E-04	
C6H8O9I	350.922	-0.07814	200	7.00E-05	

Figure S1: Proposed reaction mechanism giving rise to the products displayed in Figure 6 (main article). The overall reaction mechanism of levoglucosan photooxidation is highly complicated, and only a subset is shown here. As one example, the mechanism demonstrates the case when H-abstraction occurs at the position shown in Scheme 1. Subsequent chain scission can lead to two different reaction pathways shown in Scheme 2 and Scheme 3, respectively. Scheme 4 demonstrates that products from Scheme 3 can undergo the hydroxyl-to-carbonyl conversion which is discussed in the functionalization section in the main article. Scheme 4 illustrates hydration of an aldehyde and its subsequent conversion to a carboxylic acid.

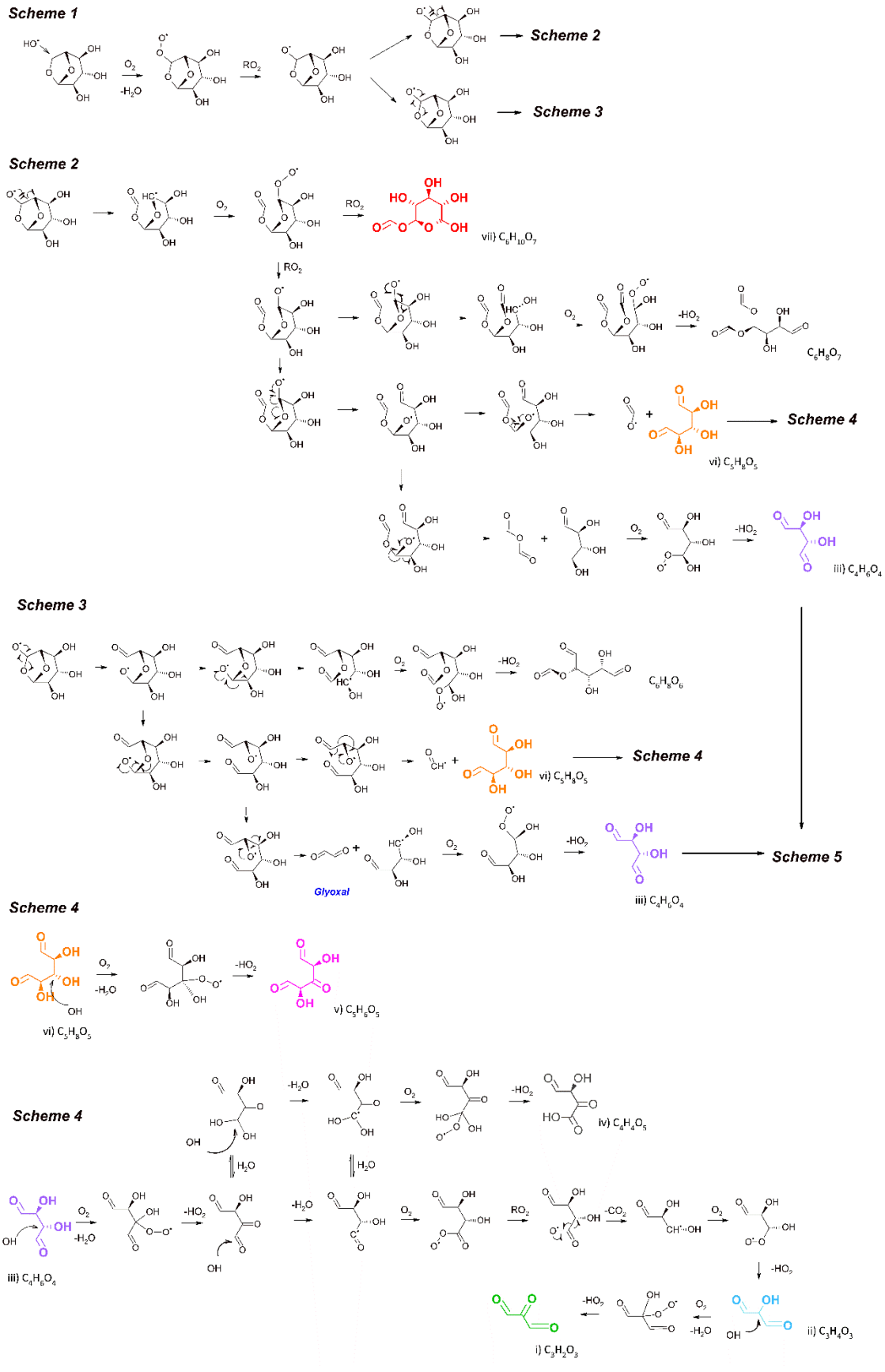
Scheme 1
Scheme 2
Scheme 3
Scheme 4
Scheme 5
vii) $C_6H_{10}O_7$
$C_6H_8O_7$
vi) $C_5H_8O_5$
iii) $C_4H_6O_4$
$C_6H_8O_6$
Glyoxal
v) $C_5H_6O_5$
iv) $C_4H_4O_5$
i) $C_3H_2O_3$
ii) $C_3H_4O_3$

Appendix S1: Estimation of the diffusion limited rate constant of LG oxidation by OH radicals in the aqueous phase.

We calculated the diffusion limited rate constant to be 1.9×10^9 $M^{-1}s^{-1}$, based on the following equation (Pilling and Seakings, 1995):

$$k\ (M^{-1}s^{-1}) = 1000 \times 4\pi \times \left(\frac{r_{LG} + r_{OH}}{2}\right) \times (D_{LG} + D_{OH}) \times N_A,$$

where 1000 is a conversion factor for units, r_x and D_x represents the radius and diffusion coefficient of molecule X in water, respectively, and N_A is the Avogadro constant. The value of r_{LG} is estimated to be 0.22 nm, assuming LG is approximately half the size of a sucrose (a sugar dimer) (Pappenheimer 1953). The value of r_{OH} is assumed to be 0.1 nm, a typical O-H bond length of a water molecule. The diffusion coefficient of glucose in water (0.6×10^{-9} $m^{-2}s^{-1}$, from Stein 1990) is used as D_{LG}, given the similarity between LG and glucose. The value of D_{OH} (1×10^{-9} $m^{-2}s^{-1}$) is adopted from Hanson et al. (1992).

References:

Hanson, D. R., Burkholder, J. B., Howard, C. J. and Ravishankara, A. R.: Measurement of Oh and Ho2 Radical Uptake Coefficients on Water and Sulfuric-Acid Surfaces, J. Phys. Chem., 96, 4979-4985, 1992.

Pappenheimer, J. R.: Passage of Molecules through Capillary Walls, Physiol. Rev., 33, 387-423, 1953.

Pilling, M. J. and Seakins, P. W.: Reaction kinetics, Oxford University Press, Oxford England ; New York, 1995.

Stein, W. D.: Channels, carriers, and pumps: an introduction to membrane transport, Academic Press, San Diego, 1990.Pilling, M. J. and Seakins, P. W.: Reaction kinetics, Oxford University Press, Oxford England ; New York, 1995.